

Implementation of a power supply with optimized voltage and power quality control by a smart filter

Adel Akbarimajd^{1,*} , Amir Mohammadhoseini Heiran² 

¹Department of Electrical and Computer Engineering, University of Moagegh Ardabili, Ardabil, Iran.

²Boston Scientific Corp, Galway, Ireland.

*Corresponding author: akbarimajd@gmail.com

Original Research

Abstract:

Received:
25 July 2024
Revised:
16 August 2024
Accepted:
2 September 2024
Published online:
15 December 2024

© The Author(s) 2024

Jet engines consume a lot of power at start time which makes it necessary to use a ground power supply unit (GPU). The GPU must provide the aircraft's demanded power at the start point only. One of the most important factors in supplying the required power for jet engines is to provide the necessary quality for the transmission of electricity to the aircraft. There are a lot of standards to check the quality of the starter among them MIL-STD-704 military standard is one of the most frequently used ones. This standard governs two principles of the power quality and transmitted power to flying vehicles. A GPU system is designed and implemented in this paper to meet the requirements of MIL-STD-704. This paper proposes a new approach to implement a starter system for turbo-shaft engines. The transformer tap changer mechanism is used for voltage control and the parameters of the transformer are also optimized using Maxwell software to reduce losses. The power quality value is achieved based on an adaptive smart filtering system implemented at the output terminal of the starter system. This smart filter is designed to be controlled based on a support vector machine (SVM) machine learning scheme. Experimental results are provided to illustrate the successful and high-quality supply of power needed to start a helicopter.

Keywords: Ground power supply; Helicopter starter; Support vector machine; Transformer design; Smart filter

1. Introduction

Aircraft systems, including helicopters, are composed of very sophisticated units, all of which are driven by electric controllers [1]. The control system in the aircraft requires a very high power that is provided by jet engines of each aircraft during flight. However, at the moment of start, when the motors are in a static state, the required power should be supplied by ground power unit (GPU) [2]. Schematic diagram of the power system of a Helicopter is shown in Fig. 1 where the starter feeds helicopter engines at the instant of start. After supplying the required power to the engines, the starter system is disconnected from the circuit and the required power is obtained from the engine generators.

The main task of each GPU is to provide the power needed to drive each engine in a nominal level. The main task of each GPU is to provide the value power needed to drive each engine in a nominal level. This value is slightly different for different types of aircrafts or helicopters, but the average

amount of power required to start an aircraft or helicopter ranges from 30 to 180 KVA [3, 4].

In order to implement a system that can deliver such a value of power, different approaches have been used namely diesel systems, batteries which are synthesized as the auxiliary power units (APUs), using electricity grid and transformer-based systems.

The use of a diesel system as a grand power supply has been very popular in the past years; those are still used in most countries [5]. In diesel systems, the voltage control is driven by a diesel generator excitation and makes a powerful controller. However, the important issue in this regard is the slow response of the system to the rapid changes of the aircraft dynamics, as the transient time of the aircraft during the start is about milliseconds and the diesel system cannot supply this level of energy at this period of time [6]. Another approach to implement the starter system using auxiliary power units (batteries). Batteries deliver an accurate voltage of 28 volts so that the system can operate

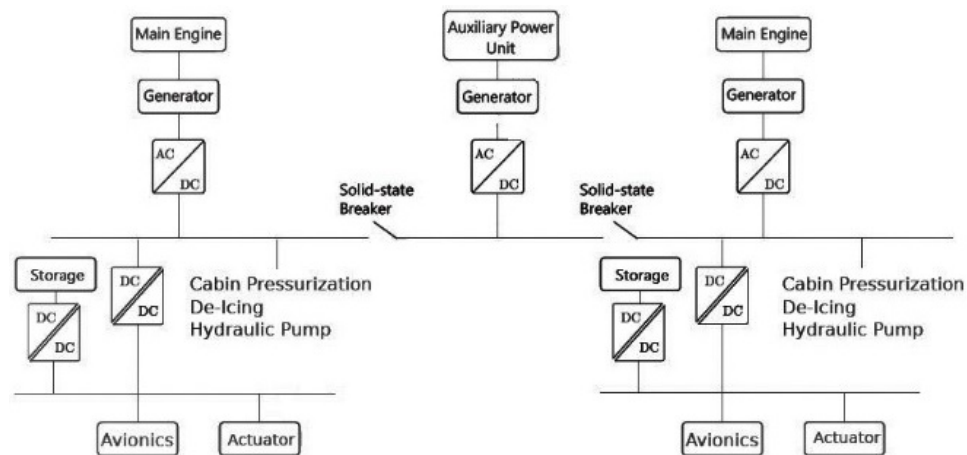


Figure 1. Helicopter power system including circuit breakers and auxiliary ground power supply unit [1].

without any voltage drop. But the batteries, based on their cellular structure, have different capacities. In the best conditions, the battery system only can start the engines 400 times, which means that the system will work not longer than one year. In addition, the shelf life of each battery in storage conditions is at most 6 months. As a result, battery-based systems cannot be used as a permanent structure [7]. One of the methods employed is to use the electricity grid to provide the power needed by the helicopter at the moment of the start [8]. In this method, the voltage level of the network should be reduced to a voltage of 28 volts, as well as converting AC to DC power. There are different ways to reduce the voltage level today, one of which is the use of power transformers. In this method, the voltage is reduced to a voltage of 28 volts and the value of power required at the start time is provided by the transformer. The main drawback of this method is that there is no voltage control, which causes 4 to 10 volts voltage decrease during start-up. The voltage drop at the start-up depends on the transformer's wiring parameters such as the diameter of the wiring, the primary and secondary wiring, and the insulation and core of the transformer [9]. The use of an auto-transformer or the use of tap-changers at the input of the power transformer reduces the level of voltage drop and the device has the ability to pass the MIL-STD-704 standard. This standard considers a voltage drop of up to 22 V [10]. In the case of using an autotransformer or using a tap-changer, the required startup power is generated, however, the power quality proposed by the standard is not operational. To achieve an acceptable power quality, a filter should be used at the output of the starter. The use of high frequency switching systems is another way to provide the power needed to start helicopters. However, these systems have the potential to damage the cold start engines due to the very low level of protection of the transient flow system [11].

Considering a variety of possible methods for implementation of a starter for helicopters, one can point out the high reliability of the transformer system. However, the existing transformer-based GPU's do not have the ability to pass the MIL-STD-704. In this paper, a voltage control system as well as a voltage quality control is applied to improve

a starter system and overcome this shortcoming. A starter system is developed which is based on the transformer structure and it is improved by voltage control and power quality systems to meet MIL-STD-704 standard. These control systems provide required output voltage based on tap changer, given device output data. Voltage control system and power quality both are matched with MIL-STD-704.

To meet MIL-STD-704 requirements, firstly the transformer core and wiring characteristics are selected using Maxwell software to reduce power loss. Secondly, a support vector machine (SVM) learning mechanism used to tune parameters of an adaptive smart filter provides the power quality required to handle nonlinear loads of flying equipment. This machine learning method improves distortion and ripple coefficient to meet MIL-STD-704 military standard. The proposed device can supply 2500 A in continuous mode with high quality output waveform. The 40 KW power required for a helicopter starter should be provided at a DC voltage of 28 V and a current of about 1500 A. In the proposed system both power generation and quality control schemes are described.

Next section introduces the building blocks of the starter and describes the design of the transformer to reduce power loss. In section 3, the details of the machine learning algorithm employed to tune the active filter is devised. Simulation and experimental results are provided in section 4 and finally the last section includes summary and conclusions.

2. Power generation system for helicopter starter

As it was discussed in the previous section, the use of a transformer for power generation is one of the most reliable methods. By installing a transformer, the required value of power can be drawn from the network. In this section, the design of the power transformer-based power generation system is devised in detail. A schematic diagram of the designed system is shown in Fig. 2.

The electrical setup includes transformer and tap changer system, an AC/DC uncontrolled converter, and an adaptive smart RC filter to power quality control. A SVM machine learning mechanism is employed to achieve an optimal

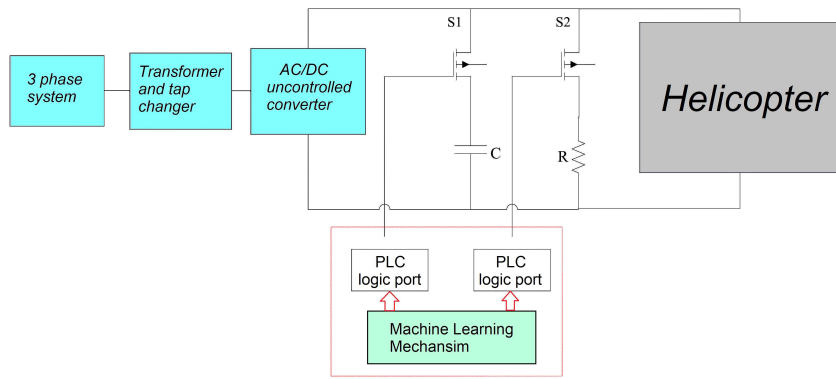


Figure 2. The starter system including transformer, tap-changer, AC/DC converter and a smart filter for power quality control tuned by SVM machine learning.

performance. Specifications of each unit of electrical setup and their design requirements are provided at the following subsections. The machine learning based smart filter, used to power quality control, is detailed in the next section.

2.1 Transformer design

It is well known that the total loss in transformers is sum of iron loss in core and copper loss:

$$P_{tot} = P_{fe} + P_{cu} \tag{1}$$

Iron loss in core and copper loss by themselves can be obtained by [12]:

$$P_{fe} = K_{fe}(\Delta B)^\beta A_c l_m \tag{2}$$

$$P_{cu} = \left(\frac{\rho \lambda_1^2 I_{tot}^2}{4K_u} \right) \left(\frac{MLT}{W_A A_c^2} \right) \left(\frac{1}{\Delta B} \right)^2 \tag{3}$$

where ΔB is the peak value of the AC component of flux density related to the applied winding voltage according to Faraday’s Law. Other parameters of equations (2) and (3) are described in Table 1. As it is obvious from (2) and (3) and their schematic illustration curves provided in Fig. 3, core loss is increased by increasing flux density and copper loss is decreased by increasing flux density. As it can be seen in Fig. 3, there is an optimized value for flux density

variation obtained from the intersection of iron losses and core losses.

Maxwell software is used to design the transformer so that the voltage drop and losses can be optimized in the system (Fig. 4). As it was explained, total power losses depend on the nature of the core and the type of transformer application. In this paper, we attempt to improve the performance of the transformer in terms of voltage drop. The characteristics of curves, hence the optimum point of total loss, depends on

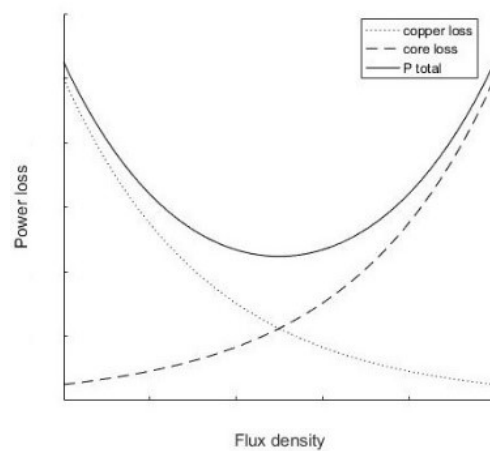


Figure 3. Power loss curves and optimized flux density of transformer.

Table 1. Parameters used in transformer design.

parameter	Sign	unit
Wire effective resistivity	ρ	(Ω -cm)
Applied pri volt-sec	λ_1	V-sec
Allowed total power dissipation	P_{tot}	W
Winding fill factor	K_u	
Core loss exponent	β	
Core loss coefficient	K_{fe}	$W/cm^3 T^\beta$
Core cross-sectional area	A_c	cm^2
Core window area	W_A	cm^2
Mean length per turn	MLT	cm
Magnetic path length	l_m	cm
Wire areas	A_W	cm^2

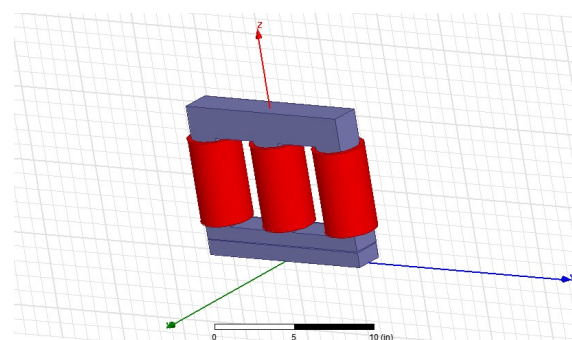


Figure 4. Three-dimensional scheme of transformer designed in Maxwell.

parameters shown in Table 1. Among them, the thickness of the core sheet, number of core sheets, type of core, and diameters of primary and secondary wiring can be designed to optimize the total loss. Using Maxwell software, one can choose appropriate values of these parameters to reduce the system voltage drop associated with the core damage of the transformer. Table 2 shows the selected values of the parameters and characteristics of the transformer. Other parameters can be selected based on [13, 14].

After simulation in Maxwell software and optimizing the materials used in the core structure as well as the designed transformer was experimentally fabricated. In Fig. 5 the physically implemented transformer as well as magnitude of the magnetic flux density of the transformer extracted from Maxwell are shown. The main purpose of designing the transformer in Maxwell is to optimize the value of magnetic flux through each core. To evaluate this, the magnitude of the magnetic flux passing through the core is shown in Fig. 5 which indicates the proper distribution of the magnetic flux in the transformer core.

2.2 Voltage control system

According to the MIL-STD-704, allowed voltage during start-up is up to 22 volts. In this paper, this voltage is set at

Table 2. Characteristics of Designed Transformer.

Description	Value
The thickness of the core sheet	0.5 mm
Number of core sheets	100
Type of core	EI 500 - Silicon
Wiring	Y
Primary wiring Diameter	3.5 mm
secondary wiring Diameter	8 mm
Insulation type	Nomex sheet
Thermal	
Number of coils turns in primary	380
Number of coils turns in Secondary	28
Final transformer dimensions	78*38*62 cm

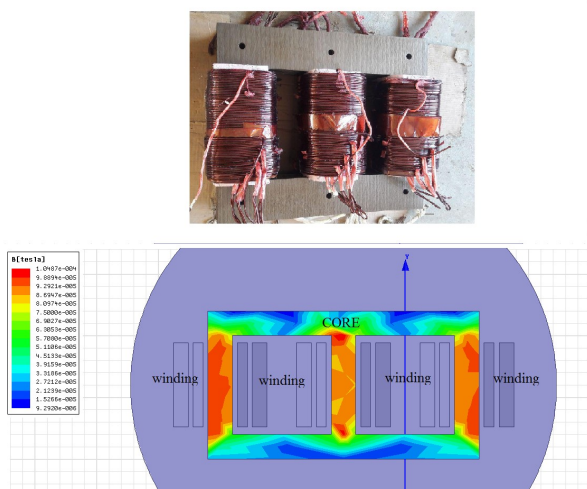


Figure 5. Transformer winding and flux density of core exported.

24 volts so that the power quality of the generator can be higher. This voltage control is based on the tap changer on the primary. For this purpose, a 3-step tap-changer system is implemented using a relay with a capacity of at least 120 A of direct current per phase. The tap changer operates such that by dropping voltage below 24 volts, a 4-volt pulse drives upwards and increases the input voltage. In this case by increasing input voltage, which is proportional to output voltage, the voltage value rises from 24 volts to 28 volts. The ratio of the change in the input and output pulse is 0.1272 per phase and 0.0736 for 3 phases. These ratios must be met at each step. This pulse control is possible by a 16-bit processor unit installed on the device. For this reason, according to the tap changer installed on the device, the system voltage is always set to 24 to 28 volts based on the MIL-STD-704.

The maximum flow rate for the input and output of the transformer is based on the mounted 3-step tap changer, for input of 120 A per phase, and for the output of the 2500 A circuit at 28 volts (see Fig. 6).

2.3 AC/DC converter

In order to convert the voltage from AC to DC mode, a three-phase full bridge rectifier has been used. In this rectifier, due to the high flow rate, two parallel diodes with a maximum allowable current of 1500 A have been used. Thus, each leg of the rectifier has withstood currents up to 3000 A. In order to reduce switching losses in diodes, the parallel snubber

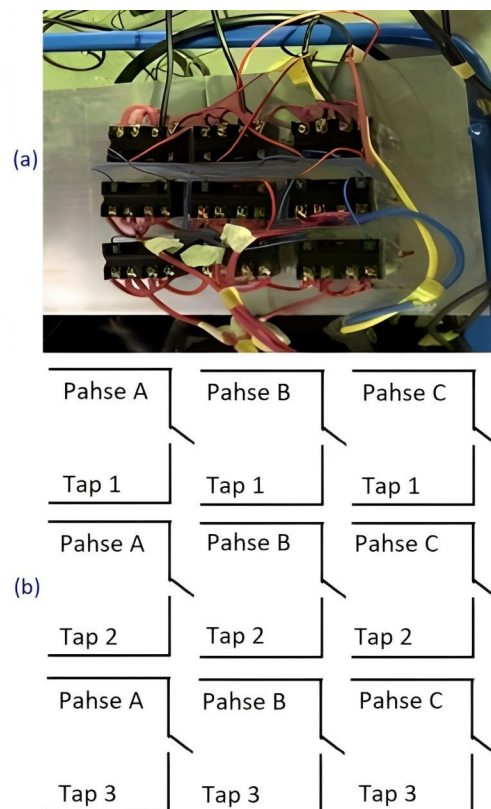


Figure 6. Tap changer system, (a) implemented setup, (b) schematic diagram: each tap can carry AC current of 100 A.

circuit board is used [15].

3. Machine learning controlled filter for power quality control

The MIL-STD-704 standard for reliability of electric power provides some rules for helicopter starters. Two factors of distortion and ripple coefficient are among the most important factors included in these rules. The max allowable ripple level for voltage of the starter system is 1.5 volts from a maximum voltage to medium voltage and minimum allowable distortion is 0.0035 (for AC starters).

In this paper in order to improve the ripple level during the starter mode, a smart adaptive filter with a SVM based machine learning controller has been used. This filter, which is shown in Fig. 2, includes a capacitor and a resistor that are controlled by two electronic switches to determine resistance and capacitance of the circuit. Due to the low flow in the parallel branch of the filter, switches with a current value of 600 A are used. The two switches are controlled by the starter CPU which is programmed based on a machine learning mechanism that changes the capacitance and resistor of the circuit according to the amount of overvoltage and the lack of voltage. The transfer function of this filter is:

$$TF = \frac{R_t}{1 + R_t C_t S} \quad (4)$$

$$R_t = e^{(-\frac{\|x_r - x_r'\|^2}{2\sigma^2})} \quad (5)$$

$$C_t = e^{(-\frac{\|x_c - x_c'\|^2}{2\sigma^2})} \quad (6)$$

where R_t is parallel resistor and C_t is parallel capacitor for output active filter.

The SVM based learning mechanism is used to tune R_t and C_t , which aims at obtaining their corresponding values and desired resistance and capacitance for achieving optimal voltage loss and ripple coefficients.

In (5) and (6), X_r is a state associated with resistive values and X_c is associated with capacitive values. σ is also introduced as the system stabilizer in the radial basis functional (RBF) equations [16]. Equations (5) and (6) characterize the SVM system which is based on the RBF kernel. In transfer function (4), R_t and C_t are unknown nonlinear functions the state of the helicopter and SVM learning mechanism is used to estimate these values. The values of R_t and C_t , are used to determine switching modes of the converter.

In order to train the SVM system, information and data corresponding to the device are firstly extracted. In order to generate the desired data, an equivalent 45-kVA inductive-resistive load with power factor of 0.7 is implemented to copy the behavior of the helicopter. Using this load equivalent circuit, the value of voltage drops and overvoltage is simulated for the device and the corresponding optimal values for the capacitor and resistance are extracted for approximately 90 samples. After extracting these 90 samples, this database is used by SVM system to estimate values of and . These values of resistance and capacitance were afterwards used to obtain the voltages applied to the gate of the power switches.

3.1 Features AC/DC converter

As it was mentioned earlier, 90 samples have been used to train learning mechanisms. These 90 samples represent system changes for different voltage drops, those are continuously modeled and experimentally recorded. These 90 samples consist of voltages and output current of the system. For this reason, two variables of the system voltage and output current are considered as the states of the learning system. With implementation of the above-mentioned load equivalent system, with a maximum tolerable current of 1400 A, different input voltages are supplied to the load equivalent circuit, in order to record output voltage and current variations. Then the learning system was trained using this data.

3.2 Normalization

Due to structural differences in two variables used for training of machine learning system and due to the different range of variations of these two features, the input data has been normalized to prevent constant convergence of the learning mechanism. There are different methods for normalization of data. In this paper, mean and the variance values of data are employed to normalize the input information as:

$$X_{norm} = \frac{X - \mu}{\sigma} \quad (7)$$

In (7), μ represents the mean value of the data, σ represents the variance value and X represents the input data associated with the 90 samples.

3.3 Kernels

The learning structure used in this paper consists of two major parts namely the cost function and the kernel. Cost functions in most of SVM based learning structures are similar with a little change, but kernels can vary desperately. The employed cost function in this paper is:

$$\min(C \sum_i y^i \cos(t_1(\theta^T x)) + (1 - y^i) \cos(t_0(\theta^T x^i) + \sum_i \theta_i^2)) \quad (8)$$

In (8), y represents the output values, x denotes input values, θ is weighted values associated with the backup method and C represents the fixed coefficient of the cost function. Radial type kernel used in the learning structure is also selected based on nonlinear behavior as the radial type is reasonably acceptable in terms of behavior [16]. Although some complex kernels could be used to increase the reliability [17] in this paler simple radial kernel was employed as it behaved well in terms of reliability and the appropriate response.

4. Simulation and experimental results

4.1 Simulations

In this section we will describe the experimental and simulation results. Aforementioned load equivalent circuit is used for extracting 90 samples to train the smart filter. A starter filter system is realized by selecting a 4700 μF capacitor and nickel chromium 2 Ω resistor. In order to properly design the filter, using the voltage-control system sampling,

the relevant information is extracted for the learning mechanism, as it is shown in Figs. 7 and 8. The SVM based machine learning algorithm was trained to generate switching signals of switches. The whole system is simulated in MATLAB-SIMULINK and the step response of output voltage with the reference value of 28 volts is shown in Fig. 9. The ripple is about 1.4% which is acceptable in MIL-STD-704 standard. Comparing the results with [18] The transient time is better (0.18sec vs 0.2sec) and the ripple value is much better (1.4% vs 4.5%). This shows that the response is acceptable according to both existing literature and MIL-STD-704 standard.

4.2 Experiments

After designing the circuit elements, optimizing core characteristics and training machine learning mechanism to tune the adaptive smart filter, the starter mechanism is physically implemented and tested on real helicopter TP-117.

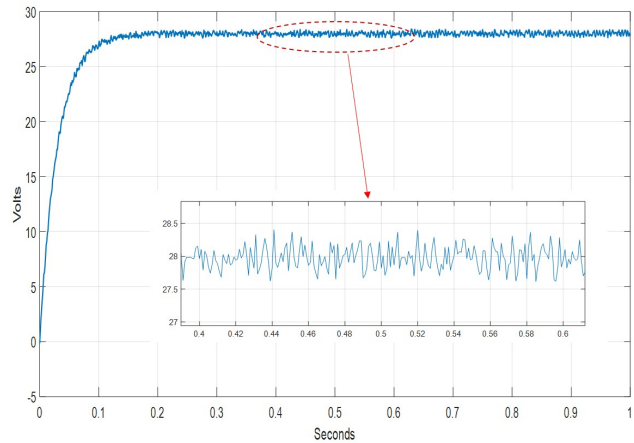


Figure 9. Step response of output voltage with the reference value of 28 volts for the designed starter system.

SKM150GAL12T4 Single IGBT Modules are used to implement switches S1 and S2. The realized starter device is shown in Fig. 10. Sampling time of the implemented system is selected as 0.5 msec. To evaluate the correctness of SVM machine learning system, the duty cycle produced by SVM is compared by above mentioned experimental results for 90 voltage current samples. Figs. 11 and 12 shows

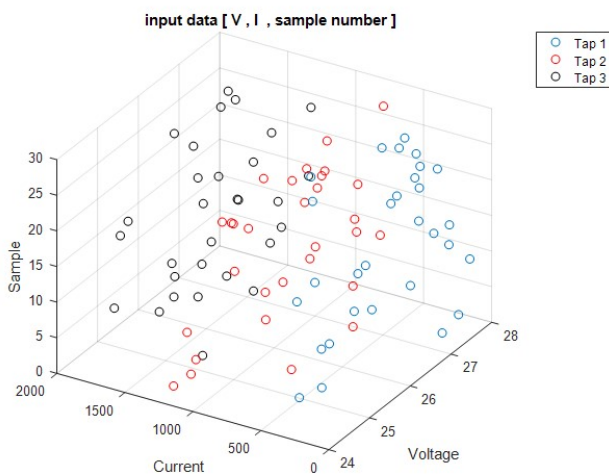


Figure 7. 90 samples of Voltage and current collected from equivalent circuit per each load.



Figure 10. Realized starter device.

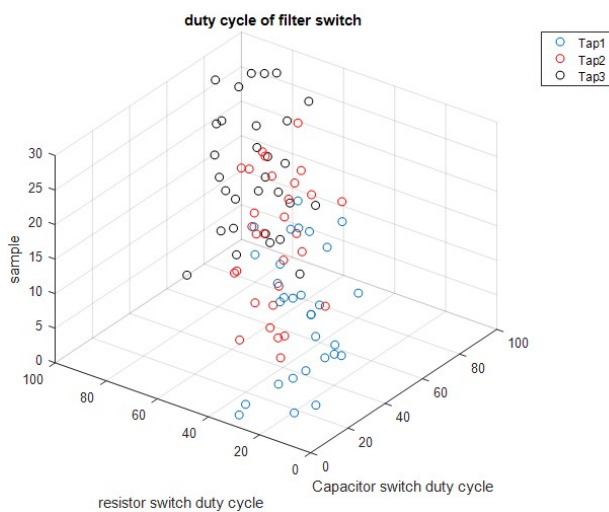


Figure 8. Training data of duty cycles of switches to control resistance and capacitance values in order to achieve appropriate power quality.

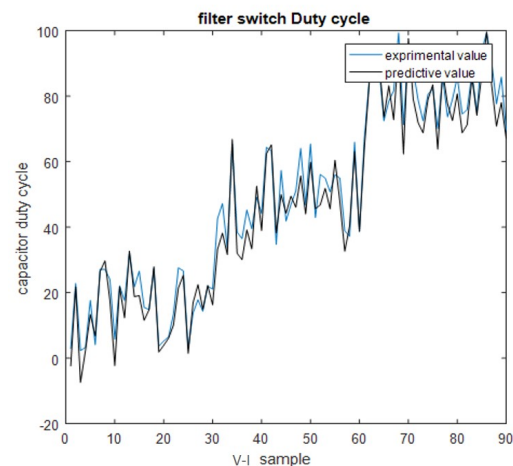


Figure 11. Capacitor switch duty cycle that applied by SVM based GPU output waveform.

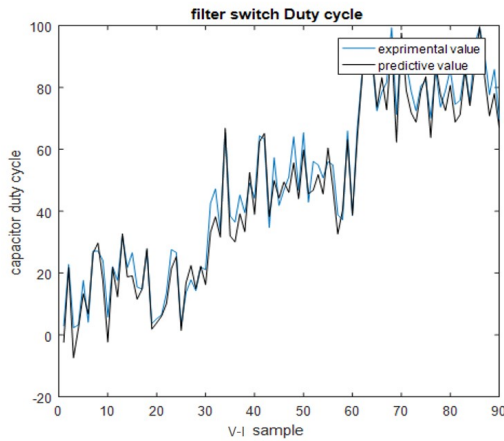


Figure 12. Resistor switch duty cycle that applied by SVM based GPU output waveform.

that machine learning has been trained well and can predict the results accurately. The output voltage of the device is recorded by a 14-bit ADC unit and the corresponding steady state is shown in Fig. 13. It can be seen that the voltage ripple is less than 1.5% which is comparable to simulation results of Fig. 9 and acceptable in MIL-STD-704.

5. Conclusion

A ground power supply system was designed and implemented for a helicopter system. Transformer tap-changer based voltage control and SVM machine learning based power quality control was used to meet MIL-STD-704 military standard. The GPU includes transformer system, voltage control unit, AC/DD converter and machine learning controlled output filter for power quality control. Parameters of the transformer were optimized using Maxwell. The transformer has multiple input taps to supply the voltage drop value. Depending on the voltage level required by the helicopter, the output voltage is set to 28 volts. Based on the transformer design, this device is capable of carrying a current of 1500 A, which

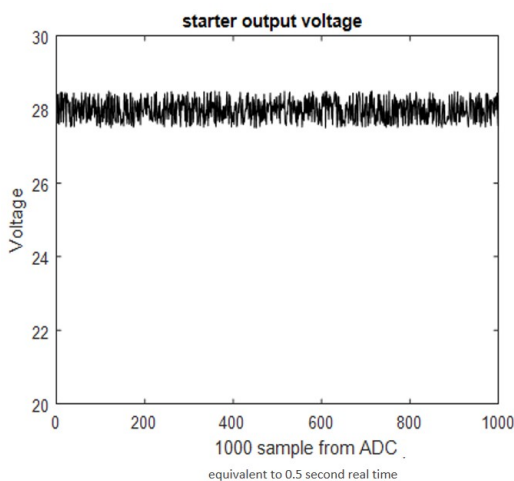


Figure 13. Steady state voltage in experimental results.

is enough for starting all types of helicopters. In order to meet MIL-STD-704 standard requirements, an adaptive smart filter controlled by an SVM based machine learning mechanism was used. This filter adjusts the capacitors and resistors needed to ensure the quality of the transmitted power. The main advantage of the present system is the use of artificial intelligence to determine filter coefficients. In addition, the optimization by Maxwell has reduced the amount of core losses in the transformer.

Authors contributions

All authors have contributed equally to prepare the paper.

Availability of data and materials

The data that support the findings of this study are available from the corresponding author upon reasonable request.

Conflict of interests

The authors declare that they have no known competing financial interests or personal relationships that could have appeared to influence the work reported in this paper.

Open access

This article is licensed under a Creative Commons Attribution 4.0 International License, which permits use, sharing, adaptation, distribution and reproduction in any medium or format, as long as you give appropriate credit to the original author(s) and the source, provide a link to the Creative Commons license, and indicate if changes were made. The images or other third party material in this article are included in the article's Creative Commons license, unless indicated otherwise in a credit line to the material. If material is not included in the article's Creative Commons license and your intended use is not permitted by statutory regulation or exceeds the permitted use, you will need to obtain permission directly from the OICC Press publisher. To view a copy of this license, visit <https://creativecommons.org/licenses/by/4.0>.

References

- [1] G. Buticchi, L. F. Costa, and M. Liserre. "Multi-port DC/DC converter for the electrical power distribution system of the more electric aircraft.". *Mathematics and Computers in Simulation*, 1(158):pp. 387–402, 2019. DOI: <https://doi.org/10.1016/j.matcom.2018.09.019>.
- [2] M. Rivera, D. Faundez, J. Kolar, P. Wheeler, F. Be-soain, and J. A. Riveros. "A New Ground Power Unit (GPU) Supply for Aircraft Applications.". *IEEE Biennial Congress of Ar-*

- gentina (ARGENCON), 6:pp. 1–6, 2018. DOI: <https://doi.org/10.1109/ARGENCON.2018.8646311>.
- [3] M. Abarzadeh and K. Al-Haddad. “An improved active-neutral-point-clamped converter with new modulation method for ground power unit application.”. *IEEE Transactions on Industrial Electronics*, 12(66(1)):pp. 203–14, 2018. DOI: <https://doi.org/10.1109/TIE.2018.2826484>.
- [4] S. L. Arevalo, P. Zanchetta, P. W. Wheeler, A. Trentin, and L. Empringham. “Control and implementation of a matrix-converter-based AC ground power-supply unit for aircraft servicing.”. *IEEE Transactions on Industrial Electronics*, 57(6):pp. 2076–2084, 2009. DOI: <https://doi.org/10.1109/TIE.2009.2034180>.
- [5] A. Selema, D. S. Osheba, S. M. Tphoon, and M. M. El-Shanawany. “Design and analysis of a three-phase brushless flux switching generator for aircraft ground power units.”. *IET Electric Power Applications*, 13(2):pp. 154–61, 2019. DOI: <https://doi.org/10.1049/iet-epa.2018.5307>.
- [6] A. C. Targino, B. L. Machado, and P. Krecl. “Concentrations and personal exposure to black carbon particles at airports and on commercial flights.”. *Transportation Research Part D: Transport and Environment*, 1(52):pp. 128–38, 2017. DOI: <https://doi.org/10.1016/j.trd.2017.03.003>.
- [7] L. Wang, Z. Zhang, C. Huang, and K. L. Tsui. “A GPU-accelerated parallel Jaya algorithm for efficiently estimating Li-ion battery model parameters.”. *Applied Soft Computing*, 1(65):pp. 12–20, 2018. DOI: <https://doi.org/10.1016/j.asoc.2017.12.041>.
- [8] J. Chen, C. Wang, and J. Chen. “Investigation on the selection of electric power system architecture for future more electric aircraft.”. *IEEE Transactions on Transportation Electrification*, 11(4(2)):pp. 563–76, 2018. DOI: <https://doi.org/10.1109/TTE.2018.2792332>.
- [9] C. R. Sarimuthu, V. K. Ramachandaramurthy, K. R. Agileswari, and H. Mokhlis. “A review on voltage control methods using on-load tap changer transformers for networks with renewable energy sources.”. *Renewable and Sustainable Energy Reviews*, 1(62):pp. 1154–61, 2016. DOI: <https://doi.org/10.1016/j.rser.2016.05.016>.
- [10] International military aviation standard. “”. *air craft electrical power characteristics S, version F*, Mil-std-704.
- [11] A. Szczepankowski and J. Szymczak. “Initiation of damage to the hot part of aircraft turbine engines.”. *Prace Naukowe Instytutu Technicznego Wojsk Lotniczych*, 38(1):61, 2016. DOI: <https://doi.org/10.1515/afit-2016-0006>.
- [12] C. W. McLyman. “Transformer and inductor design handbook.”. *CRC press*, 31, 2004. DOI: <https://doi.org/10.1201/9780203913598>.
- [13] J. Casmero and R. Barden. “FEATURES-Transformer Bobbin and Core Selection Involves Interdisciplinary Design and Cost Issues-Transformer core and bobbin selection go hand-in-hand.”. *PCIM Power Electronic Systems*, 26(10):pp. 20–35, 2000.
- [14] E-Core and Lamination Size Cross Reference. “”. URL <https://www.lodestonepacific.com/wp-content/uploads/2021/08/Bobbin-E-Core-Lam-Cross-Reference.pdf>.
- [15] H. Zhang, B. Kou, L. Zhang, and Y. Jin. “Digital controller design based on active damping method of capacitor current feedback for auxiliary resonant snubber inverter with LC filter.”. *Applied Sciences*, 22(6(11)):377, 2016. URL [10.3390/app6110377](https://doi.org/10.3390/app6110377).
- [16] M. Ring and B. M. Eskofier. “An approximation of the Gaussian RBF kernel for efficient classification with SVMs.”. *Pattern Recognition Letters*, 1(84):pp. 107–13, 2016. DOI: <https://doi.org/10.1016/j.patrec.2016.08.013>.
- [17] Y. Tan and J. Wang. “A support vector machine with a hybrid kernel and minimal Vapnik-Chervonenkis dimension.”. *IEEE Transactions on knowledge and data engineering*, 3(16(4)):pp. 385–95, 2004. DOI: <https://doi.org/10.1109/TKDE.2004.1269664>.
- [18] M. Abarzadeh and H. M. Kojabadi. “A static ground power unit based on the improved hybrid active neutral-point-clamped converter.”. *IEEE Transactions on Industrial Electronics*, 21(63(12)):pp. 7792–803, 2016. DOI: <https://doi.org/10.1109/TIE.2016.2557314>.